

Guided-mode resonance sensor with extended spatial sensitivity

David Fattal^a, Mike Sigalas^a, Anna Pyayt^{a,b}, Zhiyong Li^a and Raymond G. Beausoleil^a

^aHewlett-Packard Laboratories, 1501 Page Mill Road, Palo Alto, CA 94304, USA

^bUniversity of Washington, Department of Electrical Engineering, Seattle, WA 98195, USA

ABSTRACT

We propose a novel design for a guided-mode resonance (GMR) grating sensor that extends the sensitivity to a large region of space, possibly several tens of microns away from the grating surface. This type of sensors has high sensitivity in the half-space above the grating, close to the theoretical limit, together with a controllable - potentially very high - quality factor. It relies on a resonance caused by a "confined" mode of a sub-wavelength thick grating slab, a mode that is largely expelled from the grating itself into the grating environment. The small thickness assumption allows us to derive a simple yet accurate analytical model for the sensor behavior, which is tested numerically using a rigorous coupled-wave analysis (RCWA) method as well as in preliminary grating transmission measurements.

Keywords: GMR sensor, gratings

1. INTRODUCTION

Sensors have many applications in everyday life, such as the detection of gases, liquids, or biological substances. Various types of resonance-based photonic sensors have attracted great interest recently, including fiber Bragg gratings,¹ planar metallic gratings,^{2,3} and planar dielectric gratings.^{4,5} These devices operate by tracking the shift $\Delta\lambda$ in resonance wavelength induced by an alteration of the optical index of the surrounding medium. The simplicity of coupling light into these sensors and the plurality of sources and photodetectors in both the infrared and the visible wavelengths make them particularly attractive. In addition, due to their compact size and their sharp spectral characteristics, these sensors can be designed to be target-specific and integrated into arrays able to sense and discriminate between a large number of analytes.

In most cases of practical interest, one can distinguish between two types of sensors: surface sensors and bulk sensors. Surface sensors are designed to react effectively to a perturbation of the surrounding medium in the immediate vicinity of the surface. By contrast, bulk sensors are designed to react to a change Δn_p in the bulk optical index n_p of the probed medium. The performance of these sensors can be assessed in terms of a normalized sensitivity

$$S = \frac{\Delta\lambda}{\Delta n_p} \frac{n_p}{\lambda}, \quad (1)$$

which has a theoretical upper limit of 1 if the dispersion of the material is neglected. In addition, the resonance linewidth λ/Q , where Q is the quality factor of the resonance, determines the minimum detectable shift in resonance wavelength. The minimum detectable shift Δn_p of a probed medium is therefore proportional to $Q \cdot S$ as long as the linewidth can be resolved by the optical detection setup.

Metallic sensors based on surface plasmon resonances can achieve great surface and bulk sensitivities since surface plasmons extend primarily outside of the metal, and propagate close to the surface. This is especially true when they are generated at wavelengths where the metal offers strong dispersion.⁶ However, metals have strong optical absorption which limits their Q , and hence the minimum detectable wavelength shift. For instance, in³ Brolo *et al.* characterized an array of nanoholes in a gold film used as a surface sensor. They reported a high bulk sensitivity $\Delta\lambda/\Delta n_p$ of 400 nm per refractive index unit (RIU), corresponding to $S \sim 0.6$, which is comparable to

Further author information: (Send correspondence to David Fattal)

David Fattal: E-mail: david.fattal@hp.com, Telephone: 1 650 587 5115

other metallic grating-based resonance devices. However, the quality factor in this metallic grating is only on the order of 20. Dielectric sensors offer much more design flexibility and can achieve extremely high quality factors, several orders of magnitude above that of their metallic counterpart. Hence when operated with a high spectral resolution optical detection setup, dielectric sensors are able to detect much smaller resonance wavelength shifts than metal sensors. However, bulk sensitivities in dielectric structures are lower than those in metal, since the optical mode participating in the resonance process must be confined inside its dielectric host, and allows only a small overlap with the probed medium. Tricks can be played to increase the mode density near a surface,⁵ but bulk sensitivities are typically poor ($S \lesssim 0.1$).

In this paper, we propose the design of planar dielectric gratings of high quality factor, with a sensitivity that reaches the theoretical limit ($S \sim 1$). The main approach we use is to reduce the thickness of the dielectric slab supporting the confined optical modes to a size much smaller than the wavelength of light. The “confined” optical modes in such structures extend significantly into the surrounding medium, which makes them very sensitive to an index change of the medium — even several microns or more away from the grating surface. These thin gratings offer several interesting properties: in addition to being extraordinarily compact, they are virtually transparent with respect to wavelengths that are only slightly detuned from their resonance. Hence, such sensors could be used as non-invasive probes of a more complex optical system.

The paper is organized as follows. We first review the physics of resonances in gratings and derive some analytical expressions corresponding to the “small thickness limit”. We are able to give closed form expressions for many properties of subwavelength-thick gratings: resonance wavelength, linewidth, spectral and spatial sensitivities. We show that thin gratings indeed achieve a value of S close to 1 and a quality factor Q that scales as t^{-3} , in practice only limited by the lateral size of the grating. We explain the difference in design between symmetric and non-symmetric gratings, the latter having a minimum critical thickness that can support a resonance. We then present some numerical results for a symmetric glass sensor, which show remarkable agreement with our predictions. Finally, we present some more numerical results on the design of a non-symmetric glass sensor on a porous glass substrate, optimized to sense an optical index change in water located in the half-space above the grating only.

2. THEORY

In-plane resonances can dramatically alter the scattering properties of planar gratings in a narrow wavelength region, and can also be very sensitive to a change in the optical index in a predefined region of space if designed properly. A particularly effective way to realize an optical sensor is to monitor the position of this type of resonance while the “probed” region of space undergoes some index change. The monitoring of the resonance can be done easily by measuring the reflection or transmission of the grating in an appropriate wavelength range. In the case of metallic gratings, the resonances are the manifestation of surface plasmons, and lead to the celebrated extraordinary transmission effect.⁷ For dielectric gratings and other photonic crystal slabs, they are the manifestation of modes confined in the slab and have been called “guided-mode resonances” (GMR).^{8,9} These resonances, both in metals and in dielectrics, are now used for many purposes, including enhanced IR spectroscopy,³ optical filters,^{8,10} and sensing.

The physics behind a resonant sensor is straightforward. The sensor is an optical structure formally described by a dielectric function $\epsilon(\mathbf{r})$ that exhibit a resonance at some wavelength λ , with a corresponding electric field profile $E(\mathbf{r})$. Here we will consider the special case of a slab of thickness t and dielectric index $n = \sqrt{\epsilon}$, placed in between a lower substrate of index $n_s = \sqrt{\epsilon_s}$ and an upper substrate also referred to as “probed region” of index $n_p = \sqrt{\epsilon_p}$ (Fig. 1).

In general, when an index change Δn_p occurs within the probed region of space Ω_p (here the upper substrate), the resonance wavelength shifts by an amount $\Delta\lambda$ given by :

$$\frac{\Delta\lambda}{\lambda} = \frac{\Delta n_p}{n_p} \int_{\Omega_p} d^3r \epsilon(\mathbf{r}) |E(\mathbf{r})|^2 \quad (2)$$

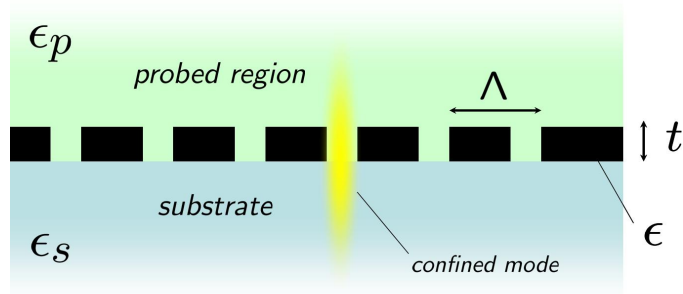


Figure 1. Generic geometry of our grating design. The probed region can be a liquid or gas, and must have a higher index than the substrate. For a symmetric grating, $\epsilon_p = \epsilon_s$.

where $E(\mathbf{r})$ has been normalized so that $\int d^3r \epsilon(\mathbf{r}) |E(\mathbf{r})|^2 = 1$ in the entire space. In terms of our normalized sensitivity, we have

$$S = \int_{\Omega_p} d^3r \epsilon(\mathbf{r}) |E(\mathbf{r})|^2, \quad (3)$$

which in particular shows that $S \leq 1$. It also hints that in order to maximize S , one wants to maximize the energy density $\epsilon(\mathbf{r}) |E(\mathbf{r})|^2$ in the probed region Ω_p . For traditional GMR structures, such as photonic crystal slabs of relatively large thickness (e.g. 200nm and above for a silicon slab at optical frequencies), this fails to be the case, since the resonant modes are mostly confined inside the slab. To remedy this problem, we propose to use a dielectric grating with sub-wavelength thickness. If designed properly, this kind of structure can expel the confined modes away from the slab and into the spatial region that needs to be probed, thus achieving high sensitivities close to the theoretical limit ($S = 1$), large quality factors, and minimal sensitivity to grating disorder and surface roughness.

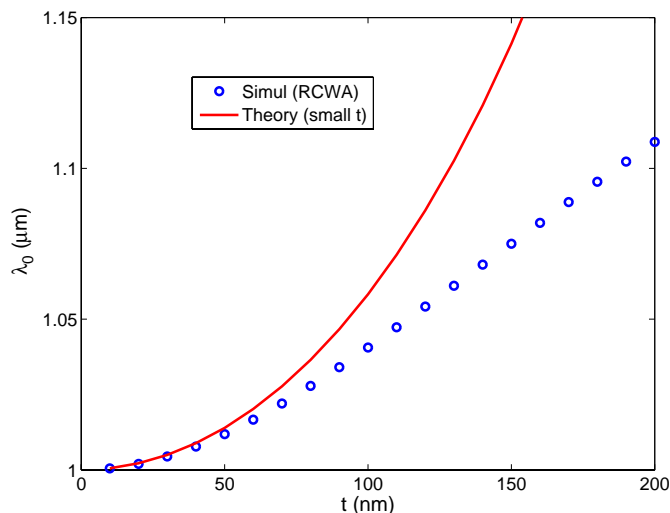


Figure 2. Plot of the resonance wavelength as a function of slab thickness for a symmetric glass grating in air. The simulation relies on the RCWA method, while the approximate theoretical curve is obtained from Eq. 8.

Returning to our three-layer geometry, we will distinguish two cases. When $\epsilon_p = \epsilon_s$, the structure has an additional mirror symmetry, and we will refer to that situation as a "symmetric slab". A symmetric slab contains a TE and TM confined mode no matter how thin, for a thickness smaller than an optical wavelength, these modes are symmetrically expelled from the slab in the substrate region. Therefore thin symmetric gratings can be expected to have high sensitivities ($S \sim .5$) on both sides of the slab. When the probed region has an index strictly greater than the lower substrate, the slab supports confined mode if its thickness t is larger than a

cutoff thickness denoted t^* which is usually itself on the order of a few or a few tens of nanometers. When $t - t^*$ is positive and small, the confined mode is again expelled from the slab, but extends exclusively in the outside region with higher index (here corresponding to the probed region – hence the name). Asymmetric gratings can therefore be expected to have high sensitivity in the probed region, with $S \sim 1$.

In what follows, we give some simple analytical formulas related to the design of symmetric and asymmetric gratings separately. Unified formulas can also be found, but they are more complex and we will omit them here.

We start by considering symmetric gratings with normalized thickness :

$$\tilde{t} = \left(\frac{\epsilon}{\epsilon_s} - 1 \right) \frac{2\pi t}{\Lambda} \quad (4)$$

We will calculate analytical expressions for various properties of the sensor in the "small thickness" limit $\tilde{t} \ll 1$, which – conveniently – is the configuration we are interested in. We assume that the confining layer is patterned in a 2D periodic way, with a square lattice of holes of index $n_s = n_p$. We will denote Λ the lattice constant of the array, by f_0 the filling fraction of the holes in the grating, and f_1 the fourier component of the grating pattern along the first reciprocal lattice vector :

$$f_0 = \frac{1}{\Lambda^2} \int_{r \in hole} d^2r \quad (5)$$

$$f_1 = \frac{1}{\Lambda^2} \int_{r \in hole} e^{-\frac{2i\pi r}{\Lambda}} d^2r \quad (6)$$

To study the resonance, we start from the knowledge¹¹ of the optical modes supported by a uniform slab, with a effective dielectric constant :

$$\epsilon_{eff} = (1 - f_0)\epsilon + f_0\epsilon_s \quad (7)$$

and study the intermixing of these modes under the perturbation introduced by the grating pattern. We find that the TE resonance occurs at a wavelength

$$\lambda_{res}^{sym} \sim \sqrt{\epsilon_s} \Lambda \left[1 - \frac{1}{8}(1 - f_0)^2 \tilde{t}^2 \right]^{-1}, \quad (8)$$

which gives a sensitivity

$$S \equiv \frac{\Delta \lambda_{res}}{\Delta n_s} \frac{n_s}{\lambda_{res}} = 1 - \frac{1}{2} \frac{\epsilon}{\epsilon - \epsilon_s} (1 - f_0)^2 \tilde{t}^2 \quad (9)$$

The above formula indeed predicts that S reaches its theoretical limit of 1 as \tilde{t} is made small (assuming that the substrate is perturbed in a symmetric way, keeping $n_s = n_p$). The mode that is excited in the resonance is well described by a profile $E(\mathbf{r})$ which is uniform in the thin slab region, and decays spatially away from the slab with inverse length

$$\kappa_{TE} = (1 - f_0) \frac{2\pi}{\Lambda} \tilde{t} \left[1 - \frac{1}{8}(1 - f_0)^2 \tilde{t}^2 \right], \quad (10)$$

Therefore rather surprisingly, the thinner the grating, the further in space it should be able to "sense".

The radiative quality factor of the resonance is given by

$$Q^{-1} = \frac{1}{2} |f_1|^2 (1 - f_0) \tilde{t}^3. \quad (11)$$

For a grating pattern consisting of a square hole of size $w\Lambda$, one can use $f_0 = w^2$ and $f_1 = \sin^2(\pi w)/\pi^2$.

These formulas are given to lowest order in \tilde{t} , and they are expected to break down as \tilde{t} approaches 1.

In the case of an asymmetric grating, the slab needs to have a minimum thickness t^* to support a confined mode.¹¹ For the TE mode, this minimum thickness is :

$$t^* = \frac{n_p \Lambda}{2\pi \sqrt{(1-f_0)(\epsilon - \epsilon_p)}} \text{Arctan} \sqrt{\frac{\epsilon_p - \epsilon_s}{(1-f_0)(\epsilon - \epsilon_p)}} \quad (12)$$

When the slab thickness t approaches the cutoff value t^* from above, the extent of the slab mode in the probed region increases. This situation is optimum for a sensor with maximum sensitivity in the upper half space. In the asymmetric case, we define a new normalized thickness by :

$$\bar{t} = \left(\frac{\epsilon}{\epsilon_p} - 1 \right) \frac{2\pi(t - t^*)}{\Lambda} \quad (13)$$

and we give simple formulas valid when $\bar{t} \ll 1$ and when the grating is asymmetric enough that :

$$\bar{t} \ll \frac{1}{2n_p} \sqrt{\frac{\epsilon_p - \epsilon_s}{\epsilon - \epsilon_s}} \quad (14)$$

In these conditions, the resonance wavelength is given by :

$$\lambda_{res}^{asym} \sim \sqrt{\epsilon_p} \Lambda [1 - (1-f_0)^2 \bar{t}^2]^{-1}, \quad (15)$$

and the (one sided) sensitivity by :

$$S \sim 1 - \frac{4\epsilon}{\epsilon - \epsilon_p} (1-f_0)^2 \bar{t}^2 \quad (16)$$

again reaching the theoretical value $S = 1$ when \bar{t} is made small. This is because for small \bar{t} , the resonant mode extends largely in the probed region, as is confirmed by the formula for its spatial decay in that region :

$$\kappa_{TE}^{asym} \sim (1-f_0) \frac{4\pi}{\Lambda} \bar{t} \quad (17)$$

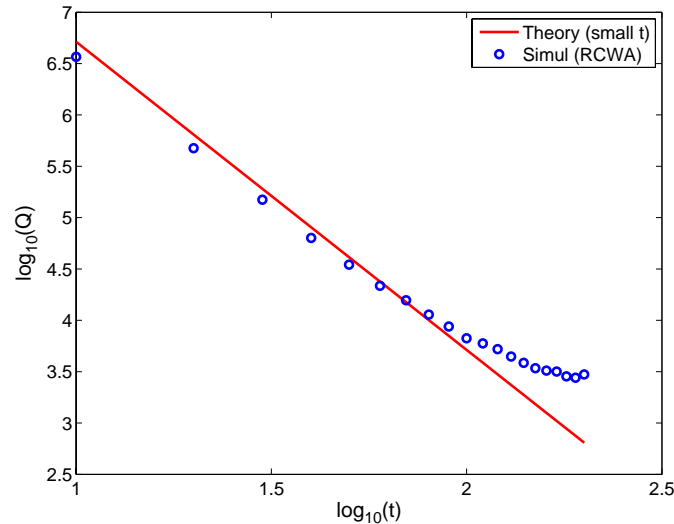


Figure 3. Plot of quality factor Q of the resonance as a function of the slab thickness t . The approximate theoretical curve is obtained from Eq. 11; we note that Q varies like t^{-3} for small t .

Before moving on to numerical simulations, we want to comment briefly on the effect of a finite grating size or illuminating beam size. The theory above strictly applies in the case of an infinite grating illuminated by a pure plane wave at normal incidence. However in practice, it is important to know – or at least estimate – how many

unit cells must be illuminated in order for our analysis to be valid. The resonance wavelength and the sensitivity S do not depend on the grating size — they are mostly determined by the dispersion of the confined mode in the unperturbed slab. However, the observed linewidths can be strongly altered by finite size effects, including a grating of finite extent and an illumination by a light beam of finite extent (or equivalently containing a range of incidence angles). A good rule of thumb that gives a slight overestimate of the required size is that the number of illuminated holes in a given direction should be on the order of the quality factor Q of the infinite grating. This corresponds to an illuminated grating area of about $(Q\Lambda)^2$. In practice, this necessary area will be smaller due to the extra lateral confinement due to the coherent backscattering of slab modes. For a thin grating sensor operating in the visible or near-IR, quality factors on the order of a thousand will be resolved for an illuminated area of about 1 mm^2 and possibly lower.

3. SIMULATION OF A SYMMETRIC GLASS GRATING

In this section, we present a numerical study of a symmetric glass grating in air. Concretely, the grating is a thin SiO_2 membrane of thickness ranging from 10 to 200 nanometers and suspended in air. We use this structure for illustrative purposes only, as we are aware that such a thin membrane could not be made of very large area with current fabrication techniques. The purpose of this exercise is rather to confront our theoretical predictions to numerical results. In the next section, we will present a more practical structure in the form of a non-symmetric grating where the confining layer lays on a solid substrate.

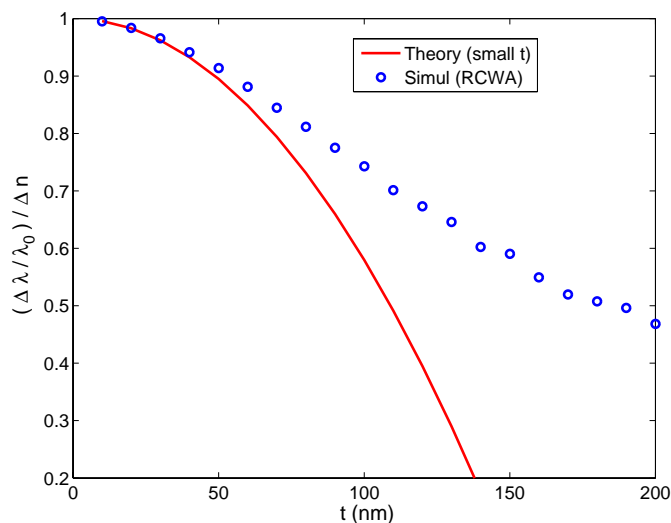


Figure 4. Plot of the normalized sensitivity S as a function of slab thickness t for the symmetric glass grating in air. The approximate theoretical curve is obtained from Eq. 9.

Our simulation relies on an RCWA algorithm using 9×9 in-plane Fourier coefficients of the grating. We use a square grating lattice of period $\Lambda = 1 \mu\text{m}$, with a square hole pattern of size $w = 200 \text{ nm}$. The values of the dielectric constant of glass were taken from¹². Around $\lambda = 1 \mu\text{m}$, glass is essentially transparent and dispersion-free. First we study the TE resonance properties of a glass grating in air, for various slab thickness. The grating is excited at normal incidence from its front side with linearly polarized light. To estimate the position and linewidth of the resonance, we look at the average field intensity on the surface of the grating, which has a familiar Lorentzian profile. It is a bit harder to get the same information from the reflection and transmission curves since they typically have Fano profiles, a signature of a resonant contribution to the far-field interfering with a non-resonant contribution. The resonance wavelength and the quality factor are shown as a function of t in figures (2) and (3), respectively, where they are compared to their predicted values. The agreement is very good for $t < 100 \text{ nm}$, and starts to break down for thicker slabs as expected. To estimate the bulk sensitivity of the resonance, we perturb the air around the grating so that $\epsilon_s = 1.001$. The corresponding normalized sensitivities are reported in figure (4). As predicted by Eq. 9, S approaches a value of 1 for small thicknesses.

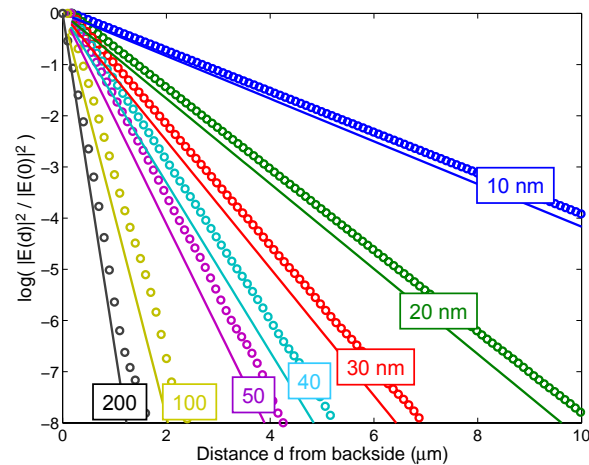


Figure 5. Simulated (o) and theoretical (-) energy density profiles away from the surface of the grating when driven on resonance. The simulation confirms the exponential spatial decay with a constant given by Eq. 10. The spatial extent of the near field is inversely proportional to the slab thickness t .

Finally the resonant near-field profiles are shown in figure (5). The figure clearly illustrates the exponential decay of the field away from the slab with a constant given by Eq. 10. As predicted, the near-field “probes” further in space as the slab thickness becomes smaller.

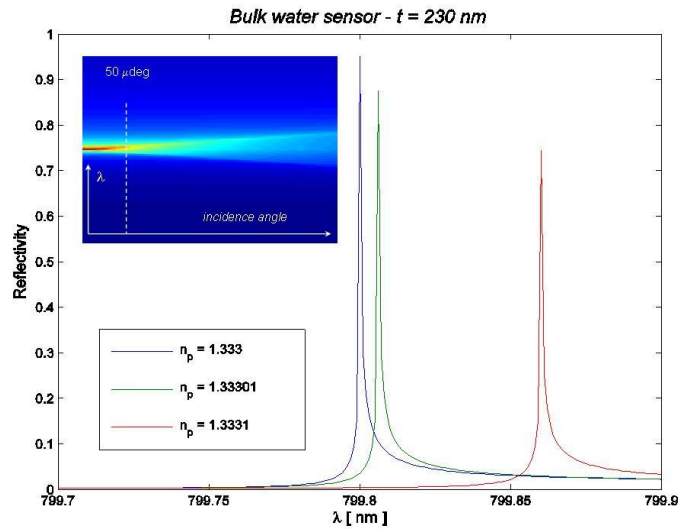


Figure 6. Reflectance of glass sensor designed to sense small shifts in the refractive index of water. The inset shows the angular dispersion of the resonance. The resonant feature is stable over a range of 50 microdegrees, corresponding to an illuminated area of about $(10 \text{ cm})^2$. The radiative Q is 8×10^5 , corresponding to a linewidth of 10^{-3} nm .

4. SIMULATION OF AN ASYMMETRIC GLASS GRATING

In order to prove that more practical designs of thin grating sensors can be realized with a non-symmetric geometry, we present the design of an asymmetric grating sensor optimized to detect an index shift in deionized water located on one side of the slab only. The goal here is to push the limits of how small an average index shift can be detected in the biggest possible area. Due to current fabrication limitations, we will assume that a periodic array can be made reliably with area greater than a few cm^2 , and we will design the sensor with that restriction in mind. We use a thin glass grating, supported by a substrate of porous glass. According to formula

(15), the resonance wavelength to zero order is given by :

$$\lambda_{res} \sim n_p \Lambda. \quad (18)$$

Here we want to create the resonance at $\lambda_{res} = 800$ nm where the index of deionized water is $n_p = 1.333$, and therefore we must choose a grating period of 600 nm. The index of glass is $n = 1.45$ and we took the index of the porous glass to be $n_s = 1.17$. We chose a square grating with circular hole features of diameter 300 nm, corresponding to a filling fraction $f_0 = 0.196$. For these values, the critical glass thickness supporting a resonance is $t^* = 223$ nm, so we choose a glass thickness $t = 230$ nm insuring high mode penetration into the water but not into the porous glass. This gives $\bar{t} = 0.014$ and an expected resonance at 799.89 nm. the result of the simulation gives $\lambda_{res} = 799.80$, and the difference is accounted for by the effect of backscattering induced by the second-order fourier coefficient of the grating which cannot be neglected here since the thickness of the slab is not small enough.

We plot the reflectance of such sensor in figure (6) for slightly varying values of the water index. We obtain a sensitivity of 599.9 nm/RIU, which corresponds to $S = 99.96\%$. The resonance is sensitive to index changes in a large region of space, as far as 10 μ m into the water in this case. From the angular dispersion shown in the inset of the figure, we estimate that the linewidth will be radiatively limited for an illuminated area of about $(10 \text{ cm})^2$. If this is the case, the linewidth will be on the order of 10^{-3} nm, corresponding to a quality factor $Q \sim 8 \times 10^5$ (which is below the absorption limit of glass at our wavelength). Putting all those numbers together, we conclude that an average index change of 10^{-6} of the water in a region extending 10 μ m above the illuminated grating area will cause a shift in the resonance corresponding to a half-linewidth. Smaller shifts could even be detected depending on the optical detection setup.

5. PRELIMINARY EXPERIMENTAL RESULTS

In this last section, we report the results of some initial measurements aiming at confirming that thin gratings can indeed support a GMR resonance, and can exhibit large sensitivities if – and only if – designed properly. The measured structures are all made out of an SOI wafer with 3μ m oxide, for which the top Si layer has been thinned to a value of 50 nm. For such a design, the silicon substrate underlying the glass layer has little effect on the silicon slab mode, and the substrate can be considered to be glass only. Using standard photolithography and dry etching, a periodic pattern was etched into the top Si layer. The periodicity of the array was designed to be 1.05μ m, giving an expected resonance λ_{res} in air around 1.5μ m. The holes were etched with varying depths and radii so that the dependence of the resonance wavelength on the filling fraction f_0 could be tested. The full results will be given elsewhere, here we merely report the measurement results for a grating with holes etched 25 nm in the silicon layer, and with different hole size (Fig. (7)). As expected, the resonance is blue-shifted as the hole size increases, and a fit to our model shows that the shift can be explained mostly by the change in the effective silicon slab index.

Next we report the measurement of one of these gratings in different environments, first in ambient air (Fig. 8) and then when immersed in a fluid that matches the index of glass (Fig. 9). When used in air, the reported sensitivity $S \sim 0.06$ is small, which is expected since most of the GMR mode is contained in the glass substrate. Even with this small sensitivity, we are able to observe the resonance shift of 0.1 nm due to the relatively large quality factor of the grating ($Q \sim 1000$).

Now when used in a liquid with index similar to the index of glass, the measured sensitivity $S \sim 0.43$ is much larger, about half the theoretical limit, which is consistent with the fact that a large fraction (about half) of the GMR mode is contained in the probed region. A more complete set of measurements will be reported elsewhere, including a series using fluids with small index increments for various hole size and depth, and another series using various incidence angles, which will test the validity of our theoretical model with more rigor.

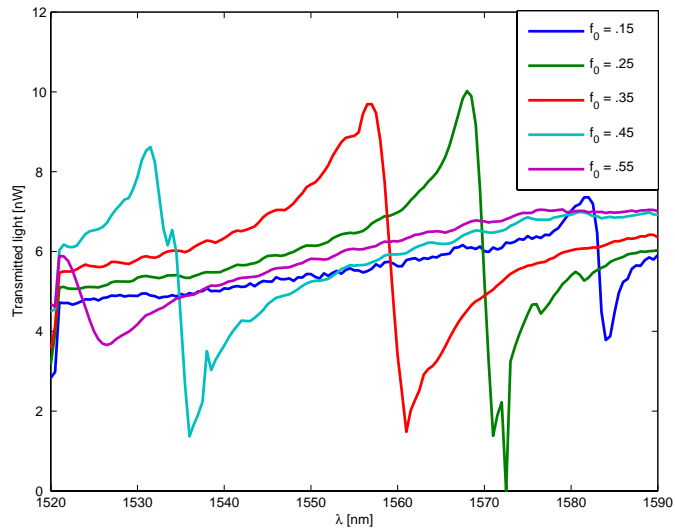


Figure 7. Measured resonance shift with hole filling fraction for a 50 nm Si grating on glass substrate in air. The holes are 25 nm deep in the Si slab. The shift is well accounted for by the change in the effective refractive index of the silicon slab due to the holes.

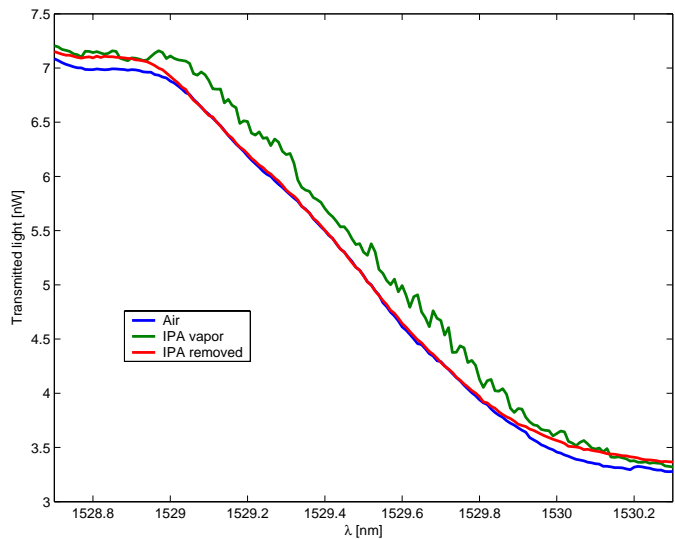


Figure 8. Measured resonance shift for a 50 nm Si grating on glass substrate in IPA saturated vapor. The shift is $\delta\lambda \sim 0.1\text{nm}$, corresponding to a sensitivity $S \sim 0.06$. This low value of the sensitivity is consistent with a resonant mode spreading mostly in the glass substrate, with only a small fraction in the air above.

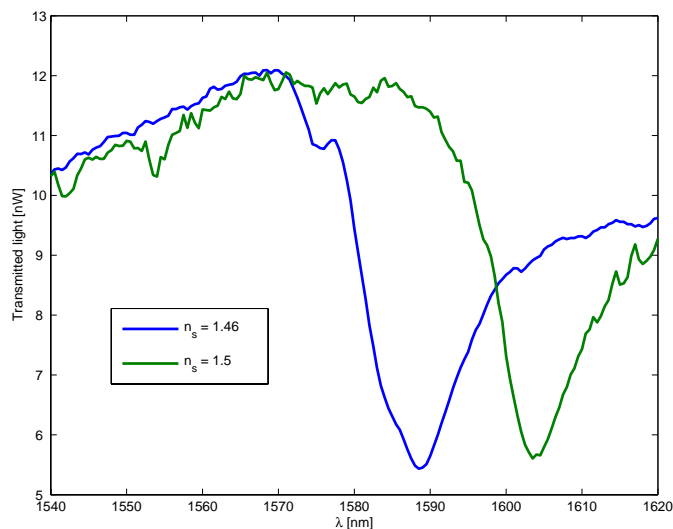


Figure 9. Measured resonance shift for a 50 nm Si grating on glass substrate immersed in index matching fluid with refractive index 1.46 and 1.5 respectively. The data give a sensitivity $S \sim 0.43$, which is consistent with a resonance mode that is spread half in the glass substrate, and half in the fluid region.

6. CONCLUSION

To summarize, we have shown how to design dielectric resonance grating sensors operating near a planar mode cutoff, providing high bulk index sensitivities, high quality factors and the ability to probe an extended region of space. The rationale for the design — the spread of a “confined” mode to an extended region of space — was first verified using numerical simulations, which confirmed that under the right design, both symmetric and asymmetric gratings could be used as sensors with sensitivities reaching the upper theoretical limit, and with very high quality factors. We also presented initial measurements for a Si sensor on glass substrate, in contact with different medium, which confirmed the theoretical and numerical predictions. Although this type of sensor could operate near any mode cutoff, we presented results using very thin slabs having only one or a few resonances. The small thickness guarantees that the radiative losses will be small regardless of the grating pattern. These structures may have potential applications as gas or liquid sensors where the probed region could extend over tens or hundred of optical wavelengths away from the surface, with detectable average index shifts of 10^{-6} or lower. They could be used with advantage for the detection of medium size particles, with sizes ranging from 1 to 10 microns, for which they would outperform traditional optical sensor with their limited spatial sensing range.

ACKNOWLEDGMENTS

We are grateful for the support of ARDA/DTO through contract no. H98320-04-C-0414.

REFERENCES

1. A. Iadicicco, A. Cusano, S. Campopiano, A. Cutolo, and M. Giordano, “Thinned fiber bragg gratings as refractive index sensors,” *Sensors Journal, IEEE* **5**, pp. 1288–1295, 2005.
2. M. U. Pralle, “Photonic crystal enhanced narrow-band infrared emitters,” *Appl. Phys. Lett.* **81**, p. 4685, 2002.
3. A. G. Brolo, R. Gordon, B. Leathem, and K. L. Kavanagh, “Surface plasmon sensor based on the enhanced light transmission through arrays of nanoholes in gold films,” *Langmuir* **20**(12), pp. 4813–4815, 2004.
4. B. Cunningham, B. Lin, J. Qiu, P. Li, J. Pepper, and B. Hugh, “A plastic colimetric resonant optical biosensor for multiparallel detection of label-free biochemical interactions,” *Sensors and Actuators B* **85**, p. 219, 2001.

5. N. Ganesh, I. D. Block, and B. T. Cunningham, "Near ultraviolet-wavelength photonic crystal biosensor with enhanced surface to bulk sensitivity ratio," *Appl. Phys. Lett.* **89**(2), p. 23901, 2006.
6. L. S. Jung, C. T. Campbell, T. M. Chinowsky, M. N. Mar, and S. S. Yee, "Quantitative interpretation of the response of surface plasmon resonance sensors to adsorbed films," *Langmuir* **14**(19), pp. 5636–5648, 1998.
7. T. W. Ebbesen, H. J. Lezec, H. F. Ghaemi, T. Thio, and P. A. Wolff, "Extraordinary optical transmission through sub-wavelength hole arrays," *Nature* **391**, p. 667, 1998.
8. R. Magnusson and S. S. Wang, "New principle for optical filters," *Applied Physics Letters* **61**(9), pp. 1022–1024, 1992.
9. M. Neviere, E. Popov, and R. Reinisch, "Electromagnetic resonances in linear and nonlinear optics: phenomenological study of grating behavior through the poles and zeros of the scattering operator," *J. Opt. Soc. Am. A* **12**, p. 513, 1995.
10. Y. Ding and R. Magnusson, "Resonant leaky-mode spectral-band engineering and device applications," *Optics Express* **12**(23), pp. 5661–5674, 2004.
11. A. Yariv and P. Yeh, *Optical Waves in Crystals*, John Wiley and Sons, Inc, Hoboken, New Jersey, 2003.
12. E. D. Palik, *Handbook of optical constants of solids*, Academic Press, San Diego, 1998.